

Optimized Damping Device Configuration Design of a Steel Frame Structure Based on Building Performance Indices

Wei Liu,^{a)} Student M.EERI, Mai Tong,^{b)} M.EERI, Yihui Wu,^{c)} M.EERI, and George C. Lee,^{d)} M.EERI

Energy dissipation devices (EDDs) have been accepted as one of the viable strategies for enhancing the seismic performance of building structures. However, the current design provisions do not provide guidelines for optimizing the EDD configurations on structures. For many building structures an efficient configuration of EDDs may provide considerable performance improvement. Similarly, an optimized configuration may reduce the number of EDDs required to achieve a target performance objective. In this paper an existing building with added linear viscous dampers is redesigned based on different performance index optimization. The results indicate that the optimal device configurations are highly related to the dynamic properties of the structure and its required performance index. In one instance, where the cost is the major concern and a performance requirement is placed on story drift limitation, the total device damping coefficient can be reduced by 26%. [DOI: 10.1193/1.1648334]

OVERVIEW OF CURRENT PROVISIONS ON BUILDING DESIGN WITH SUPPLEMENTAL EDD

Two design provisions are available for designing structures with added energy dissipating devices (EDDs). *FEMA-356 (Prestandard and Commentary for the Seismic Rehabilitation of Buildings)* (ASCE 2000), updated from *FEMA-273 (ATC 1997)*, provides guidelines for the application of EDDs to rehabilitate existing buildings based on defined rehabilitation objectives. *FEMA-368 (NEHRP 2000 Recommended Provisions for Seismic Regulations for New Buildings and Other Structures)* (BSSC 2001) provides a design procedure for new building structures with added EDDs.

FEMA-356 specifies four analysis methods for buildings retrofitted with added EDD. They are linear static, linear dynamic (including the response spectrum method), nonlinear static, and nonlinear dynamic procedures. To account for the damping from added EDDs, a damping modification factor is used to reduce the seismic effect on the struc-

^{a)} Graduate Research Assistant, Civil, Structural & Environmental Engineering Dept., University at Buffalo, Buffalo, NY 14260

^{b)} Senior Research Scientist, Multidisciplinary Center for Earthquake Engineering Research (MCEER), University at Buffalo, Buffalo, NY 14260

^{c)} Senior Structural Engineer, Maguire Group, 225 Chapman St., Providence, RI 02905

^{d)} Samuel P. Capen Professor of Engineering and Special Tasks Director of MCEER, University at Buffalo, 429 Bell Hall, Buffalo, NY 14260

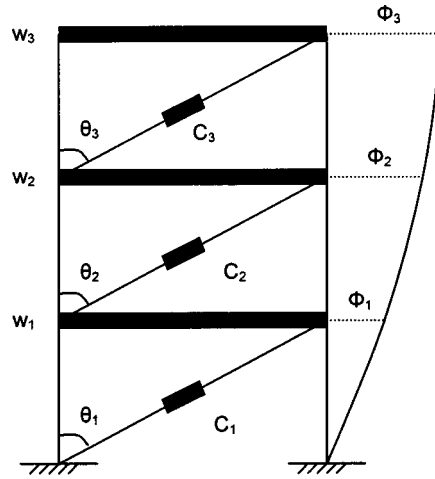


Figure 1. Elevation view of a building with EDDs.

ture. In the linear static procedure, the pseudo lateral load in a given horizontal direction is reduced. In the response spectrum method, the 5%-damped design response spectrum is modified. In the nonlinear static procedure, the spectral acceleration should be reduced for velocity-dependent EDDs. The damping modification factor comes from the estimated effective damping ratio β_{eff} .

$$\beta_{\text{eff}} = \beta + \frac{\sum_j W_j}{4\pi W_k}, \quad (1a)$$

where β is the inherent damping in the structural frame, generally 5%. (The structural nonlinear behavior is not considered in the linear procedures, it is considered in the nonlinear static procedure by force-displacement curve instead of damping.) W_j is the work done by device j in one complete cycle corresponding to floor displacements, and W_k is the maximum strain energy in the frame. For a structure with only linear viscous devices, the effective damping can also be obtained by

$$\beta_{\text{eff}} = \beta + \frac{\sum_j C_j \cos^2 \theta_j \phi_{rj}^2}{2\omega \sum_i \left(\frac{w_i}{g}\right) \phi_i^2}, \quad (1b)$$

where C_j is the damping constant of device j , shown in Figure 1, θ_j is the angle of inclination of device j to the horizontal, ϕ_i is the first-mode displacement at floor level i , and ϕ_{rj} is the first-mode relative displacement between the ends of device j in the horizontal direction. ω is the fundamental frequency of the building including the stiffness of the velocity dependent devices, w_i is the weight at floor level i .

For new buildings, *FEMA-368* adopts the same philosophy as *FEMA-356* for the

structural design and analysis with added EDDs. For the equivalent lateral force and response spectrum analysis procedures, the seismic force-resisting system is designed using a modified base shear considering effective damping.

Both design provisions are based on a performance-based design methodology, which is considered to be the next generation of structural engineering practice. It is intended to allow construction with predictable seismic performance and to provide owners and designers with the capability of selecting alternative performance goals for the design of different buildings. Design engineers can select the target building performance level as the permissible damage to the structural elements (often related to the force or acceleration) and the permissible drift. Depending on the structure, some performance requirements can be more stringent than others. The most stringent requirement may be taken as the primary performance index, and the indexed performance is reduced to an acceptable level by adding EDDs.

Both provisions, *FEMA-356* and *FEMA-368*, adopt effective damping in the commonly used design procedures. Using these provisions, the design starts with a design requirement (e.g., reduce the base shear or drift by 30%). The effective damping ratio is estimated from the relationship between the damping modification factor (reduction ratio) and effective damping. Then, using Equation 1a or 1b, the damping coefficient for each device is estimated to achieve the desired effective damping. The members of the structure are then designed with the modified base shear for strength.

Although the above design approach can provide the structure with acceptable response reduction, it does not guarantee optimal performance. Furthermore, the effect of different performance indices used in the response reduction is not addressed. The optimal device configuration might be different if the performance index is selected differently. In order to investigate the optimal device configuration design, a building designed with EDDs is taken as a case study. The existing EDD configuration is optimized for different performance indices.

OVERVIEW OF DEVICE CONFIGURATION OPTIMIZATION

The supplemental EDDs are known to enhance the performance of the building. It is also known that the configuration of EDDs has a significant effect on the structural dynamic behavior under earthquake excitations. Many researchers realized the importance of optimal device placement, even before the EDD was included in the design provisions. There are several parametric studies on the effect of damper capacity and location. For example, Chang et al. (1995) investigated the seismic behavior of a steel frame structure with added viscoelastic dampers. Hahn and Sathivageeswarm (1992) showed that dampers should be placed in the floors in the lower half of the building if it is of uniform story stiffness. Because these studies always use simple and regular structures, they are not exhaustive and their results cannot be used as criteria for optimization.

Some recent publications addressed optimal capacity of EDDs based on the analytical optimization approach. The objective functions and the constraints (generally, the total damping capacity) are defined first. The analytical objective function is then optimized. Different objective functions are adopted in these studies. The objective function can be the maximum displacement under white noise motion (Constantinou and Tadjba-

khsh 1983), energy (Gurgoze and Muller 1992), system response and control gain matrix (Gluck et al. 1996), pre-assigned modal damping and natural frequency (De Silva 1981), norm of the transfer function (Spencer et al. 1994, and Takewaki 1997), total story stiffness (Tsuji and Nakamura 1996), or the desired level of response reduction (Singh and Moreschi 2001). The limitation of these general approaches is that the response to an arbitrary ground motion cannot be defined as an analytical objective function. Also, the results of device sizing may not be practical for commercial products.

There are some other studies using heuristic approaches to obtain the optimal placement and capacity of the devices. Zhang and Soong (1992), Wu et al. (1997), and Shukla and Datta (1999) proposed and extended the sequential seismic design method to find the optimal configuration of viscous dampers for buildings with specified story stiffness. Their contribution is based on the intuitive criterion that additional damping should be placed sequentially on the story with the maximum interstory drift. Lopez Garcia (2001) simplified this approach and showed its effectiveness on drift response. Using a similar heuristic, Agrawal and Yang (1998) investigated the optimal location of an energy dissipation system using search techniques. These heuristic approaches are practical, and they can effectively improve the structure performance with respect to story drift. These approaches do not, however, guarantee the global optimum. Furthermore, the results from Singh and Moreschi (2001) showed that the sequential approach by Zhang and Soong obtains very low response reduction for acceleration response, especially for a building with non-uniform story stiffness.

Evolutionary approaches (e.g., genetic algorithms) are used in some studies to optimize the device configuration. Singh and Moreschi (1999) used a genetic algorithm to obtain the optimal configuration of EDD devices on a structure for a desired level of response reduction. These probabilistic-based approaches can converge to the optimal configuration given enough iteration. However, these approaches are limited because they are computation intensive and time consuming.

These previous research efforts establish a foundation for EDD configuration optimization research. However, there are some important issues that still must be addressed. For example, none of these efforts addresses the performance requirements sufficiently to ensure that an optimal configuration is obtained for a given performance index and a building structure. Many of them cannot be integrated with current design procedures. In the following case study we shall investigate these issues.

THE CASE-STUDY BUILDING STRUCTURE

This case study is based on an 11-story, pyramid-shaped, steel frame structure. There are also several concrete columns on the first three stories of the building. The building height is 48 m (156 feet). The plan area is $90 \times 90 \text{ m}^2$ ($300 \times 300 \text{ ft}^2$) at the ground level and $36 \times 27 \text{ m}^2$ ($120 \times 90 \text{ ft}^2$) at the top (see Miyamoto and Scholl 1996). The building view and the 3-D structural frame are shown in figures 2 and 3. The first-floor plan and north-south, east-west elevations are shown in Figure 4.

A finite element (FE) model of the structure is formed in SAP2000 using the structural design drawings. Frame elements are used to represent the columns and the beams specified in the drawings. The mass of the building is distributed over the joints accord-

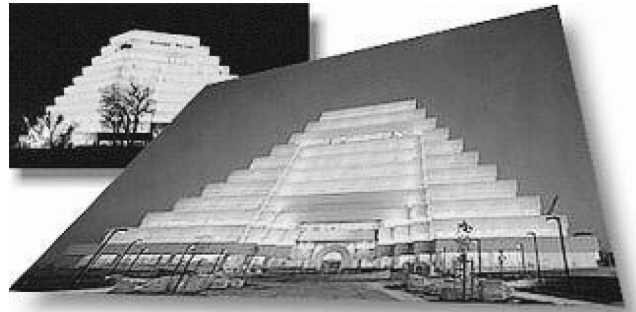


Figure 2. View of the case study building.

ing to their tributary area of the dead load and participating live load. Based on the *ASCE 7-98* design code (ASCE 1998), the dead load includes the weight of walls, floors, ceilings, partitions, and other architectural items. The live load is defined as 2.4 kN/m^2 (50 psf) for office use, with 0.5 kN/m^2 (10 psf) considered as participating mass of the structure per *ASCE 7-98*. The structure is assumed to be rigidly restrained on the foundation. The model mesh is shown in Figure 3.

For computational efficiency, the original SAP2000 model is simplified by dividing it into three parts: one part for the left wing, one for the right wing, and one for the middle. On each story there are three lumped masses, one for each part. On the 11th story, where the area is small, only two lumped masses are considered. The lumped mass model is shown in Figure 5 and the mass distribution of the lumped masses is shown in Table 1. To accurately represent the SAP2000 FE model by the lumped mass model, the stiffness of the simplified model is derived from the FE model using flexibility analysis. For each degree-of-freedom (DOF) i , a unit force $f_i = [0 \dots 1 \dots 0]^T$ is applied on the i th

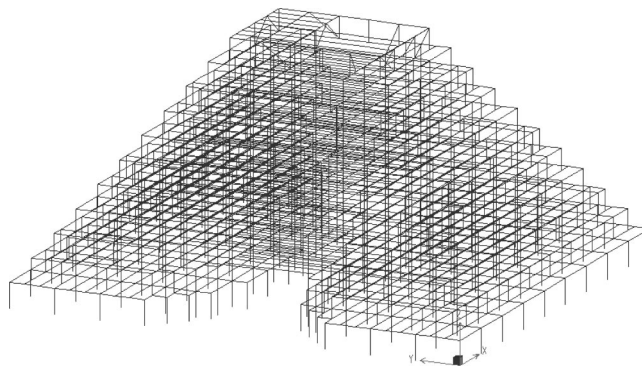


Figure 3. 3-D structural frame of the case study building.

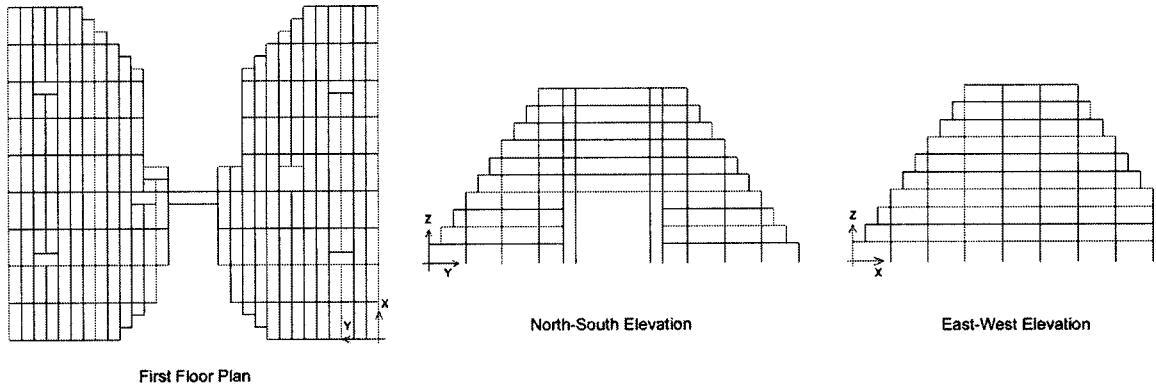


Figure 4. Floor plan and elevation of the building.

DOF. The displacement at all the DOFs corresponding to this unit force is $X_i = [x_1 \dots x_i \dots x_n]^T$. The force matrix $F = [f_1 \dots f_i \dots f_n]$, and the displacement matrix $X = [X_1 \dots X_i \dots X_n]$ satisfy the following equation:

$$F = KX \quad (2)$$

The stiffness matrix K can be obtained by multiplying F to the inverse of the displacement matrix X . The stiffness distribution obtained for the lumped mass model is

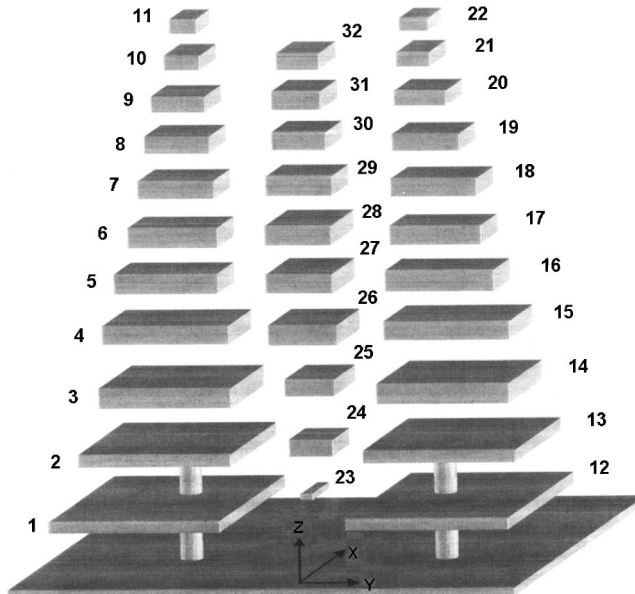


Figure 5. Simplified model of the structure.

Table 1. Mass distribution at each DOF of the simplified model

Story	DOF	Mass (1000 kg)		Mass (1000 kg)		Mass (1000 kg)		Mass (1000 kg)		Mass (1000 kg)		
		DOF	DOF	DOF	DOF	DOF	DOF	DOF	DOF	DOF	DOF	
1	1	796	12	796	23	9	33	796	44	796	55	9
2	2	585	13	585	24	121	34	585	45	585	56	121
3	3	541	14	541	25	132	35	541	46	541	57	132
4	4	458	15	458	26	239	36	458	47	458	58	239
5	5	381	16	381	27	226	37	381	48	381	59	226
6	6	282	17	282	28	200	38	282	49	282	60	200
7	7	218	18	218	29	178	39	218	50	218	61	178
8	8	165	19	165	30	147	40	165	51	165	62	147
9	9	119	20	119	31	147	41	119	52	119	63	147
10	10	74	21	74	32	121	42	74	53	74	64	121
11	11	84	22	59			43	84	54	59		

Note: DOF 1~32 are in x -direction, and DOF 33~64 are in y -direction.

shown in Table 2. To be certain that the reduced DOF model has structural dynamic characteristics close to those of the FE model, the structural characteristics of the two models are compared in Table 3. Because the structure is more rigid in the y -direction, most of the low-frequency modes are in the x -direction. Note that the simplified model captures most of the significant modes. For modes higher than the 10th mode, the SAP2000 model has a lot of local modes that are not included in the simplified model. The mode shapes of the two significant modes are compared in Figure 6. Table 3 and Figure 6 show that the simplified model closely represents the SAP2000 FE model. This is also proved by Figure 7, which plots the maximum roof displacement under the El Centro ground motion.

Table 3 also lists the mass participation ratio for each mode. This ratio, defined as the percentage of total mass in each mode, is calculated from Equation 3. Due to the normal property of the mode shapes, for each direction, the sum of the mass ratio from all contributing modes is 100%.

$$mass_ratio_i = \frac{(\text{diag}(M)\Phi_i)^2}{\sum_{k=1}^n M_{kk}} \quad (3)$$

PERFORMANCE OF THE STRUCTURE WITHOUT ADDED DEVICE

In this case study a design response spectrum is used as a representation of possible earthquake load applied to the structure. The design spectrum is constructed following the *FEMA-356* prestandard for the building site. The acceleration parameters are selected from the seismic map and the soil condition is rock. The seismic hazard level is Basic Safety Earthquake-1 level (BSE-1, earthquake has a 10% probability of exceedance in 50 years). For the time-history analysis, three artificial earthquake records are required by the standard. For this study, the artificial ground accelerations are obtained by modifying the frequency contents of actual earthquake records, so that the response

Table 2. Stiffness distribution between DOFs for the simplified model

story	DOF-DOF	K (N/m)	DOF-DOF	K (N/m)	DOF-DOF	K (N/m)
1	G-1	1.87E+09	G-12	1.78E+09	G-23	1.35E+05
2	1-2	1.58E+09	12-13	1.57E+09	23-24	9.01E+06
3	2-3	1.45E+09	13-14	1.45E+09	24-25	9.23E+06
4	3-4	1.02E+09	14-15	1.01E+09	25-26	1.15E+07
5	4-5	4.38E+08	15-16	4.39E+08	26-27	1.11E+07
6	5-6	4.34E+08	16-17	4.35E+08	27-28	1.01E+07
7	6-7	3.60E+08	17-18	3.61E+08	28-29	9.19E+06
8	7-8	2.52E+08	18-19	2.53E+08	29-30	8.25E+06
9	8-9	2.38E+08	19-20	2.39E+08	30-31	8.25E+06
10	9-10	1.71E+08	20-21	1.64E+08	31-32	2.35E+07
11	10-11	3.47E+07	21-22	4.95E+07		
1	G-33	2.43E+09	G-44	2.41E+09	G-55	2.18E+08
2	33-34	3.72E+09	44-45	3.47E+09	55-56	3.00E+09
3	34-35	5.21E+09	45-46	5.19E+09	56-57	2.39E+09
4	35-36	1.10E+10	46-47	1.00E+10	57-58	9.77E+09
5	36-37	6.58E+09	47-48	6.21E+09	58-59	5.31E+09
6	37-38	5.67E+09	48-49	5.38E+09	59-60	4.57E+09
7	38-39	4.65E+09	49-50	4.52E+09	60-61	3.90E+09
8	39-40	3.89E+09	50-51	3.58E+09	61-62	3.28E+09
9	40-41	3.84E+09	51-52	3.58E+09	62-63	3.07E+09
10	41-42	4.05E+09	52-53	3.62E+09	63-64	1.78E+09
11	42-43	6.35E+08	53-54	6.39E+08		

Note: The stiffness matrix of the simplified model is a full matrix due to the flexibility analysis method. This table only shows the significant diagonal portion.

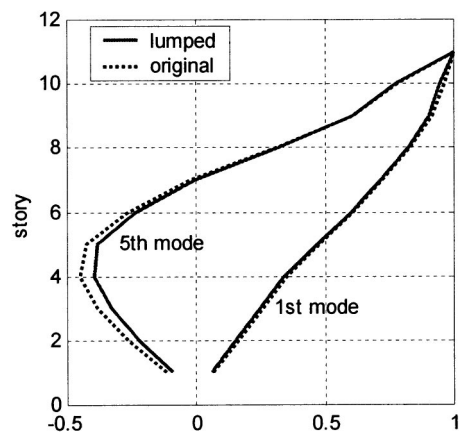
spectra are compatible with the design spectrum. The original records are taken from the El Centro (1940), Kobe (1995), and Northridge (1994) earthquakes, respectively. The response spectra of the modified records, together with the design spectrum, are plotted in Figure 8. The peak ground accelerations of these three artificial records are 0.396 g, 0.583 g, and 0.44 g, respectively.

The maximum responses of the structure subjected to the design earthquakes are plotted in Figure 9. Since this study is limited to x -direction, only the response in the x -direction is plotted. Among all the DOFs, the maximum drift occurred at the middle part of the building, where the degrees-of-freedom varied from 23 to 32. The drifts at these locations are much larger than the drifts at other DOFs. This is because the earthquake excites the third mode, which is a local mode due to the lateral vibration of the long beams. Note that the mass at these DOFs is small (e.g., the mass at DOF 23 is only 1% of the mass at DOF 1). Although this local effect may be important under certain situations (earthquake has a very large frequency component at the third modal frequency), it does not affect the integrity of the building. The purpose of including these DOFs in the simplified model is to capture the local modes provided in SAP2000 model, and to give close representation of the detailed model.

Table 3. Comparing the dynamic characteristics of the structure in the simplified model and the original FE model (assume 3% structural damping)

mode	Lumped mass model				Original SAP2000 model			
	natural freq. (HZ)	direction	mass ratio %	Mode shape	natural freq. (HZ)	direction	mass ratio %	Mode shape
1	0.655	X	64	T	0.584	X	65.00	T
2	0.701	Y	64.94	T	0.636	Y	65.47	T
3	0.895	X	0.08	L	0.825	X	0.13	R
4	1.055	X	2.44	R	0.841	X	0.07	L
5	1.291	X	10.5	T	1.188	X	12.65	T
6	1.528	X	0.82	L	1.359	X	1.20	R
7	1.546	Y	16.64	T	1.430	Y	15.10	T
8	1.566	X	0	L	1.475	X	0.30	L
9	1.598	X	0	L	1.520	X	0.00	L
10	1.663	X	0	L	1.555	X	0.00	L
11	1.724	X	4.97	T	1.569	X	0.48	R
12	1.818	X	0.1	L	1.615	X	0.05	L
13	1.896	X	0.36	R	1.682	X	3.84	T
14	1.974	X	0.23	L	1.731	X	0.22	L
15	1.996	X	2.18	T	1.874	X	0.34	L
16	2.51	Y	8.42	T	1.897	X	0.12	L
17	2.625	X	0.05	T	1.910	X	0.22	L
18	2.953	X	2.45	R	1.947	X	1.63	L
19	3.353	X	1.11	T	2.046	X	0.27	L
20	3.686	X	2.1	T	2.081	X	0.00	L

Note: Mode shape “R” means rotational mode, “T” means translational, and “L” means local.

**Figure 6.** Mode shapes comparison between the simplified model and the original FE model.

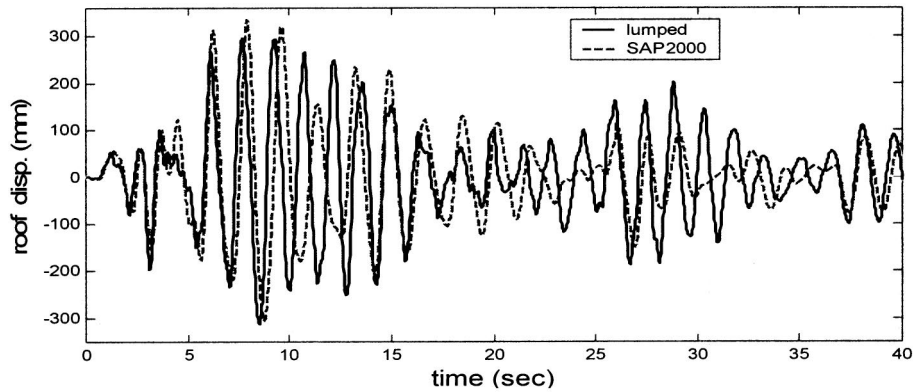


Figure 7. Seismic response comparison between the simplified model and the SAP2000 FE model.

Because of the architectural feature of the building, the local vibration effect at DOF 23 to 32 is not controllable. Also, because the third mode is isolated and the damage of this long beam will not affect the whole building, the responses at DOF 23 to DOF 32 are not considered further. In addition, due to the diaphragm constraint, only one response quantity is needed for each story. Therefore, in the remainder of this paper, only the story responses are considered. Each of the story responses is the larger response of the two corresponding degrees-of-freedom.

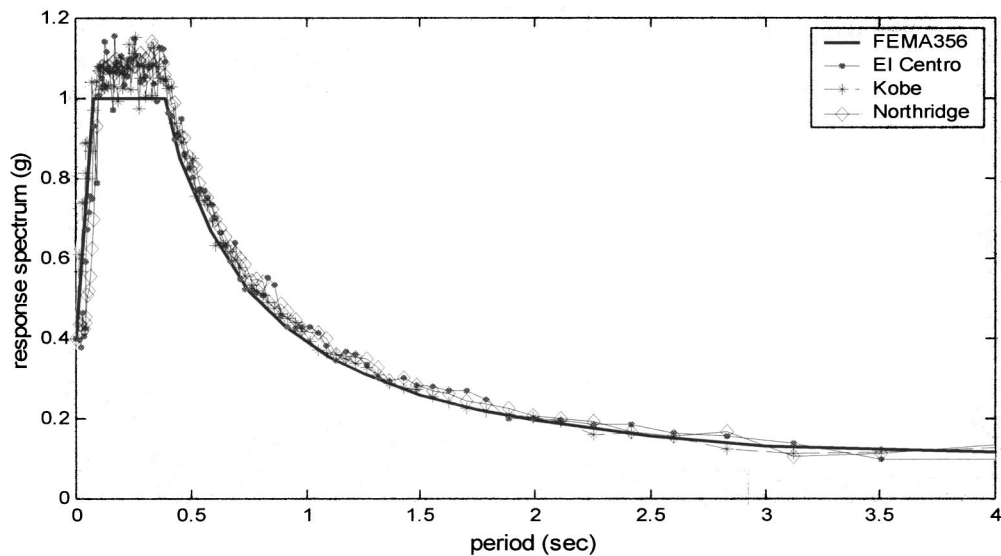


Figure 8. The design response spectrum and the response spectra of the artificial earthquakes.

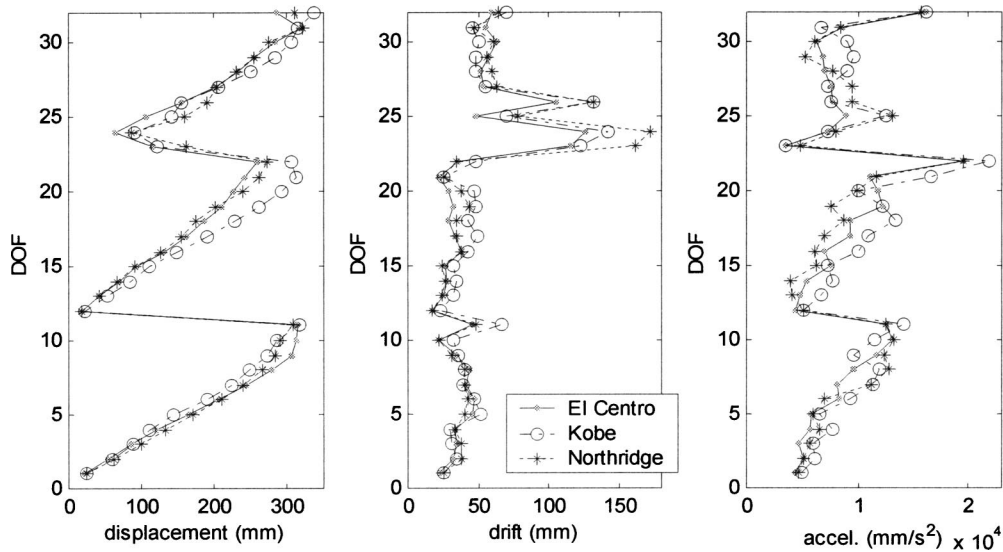


Figure 9. The maximum response in x -direction.

DEVICE CONFIGURATION I: VISCOUS FLUID DAMPERS

The building in this case study was originally designed with added bracing-type EDDs. The design objective is to achieve the owner-specified performance level at BSE-1 level earthquakes. This design objective is more stringent than life safety under BSE-1 level to protect the welded moment connections and the exterior glass decoration. The story drifts of the structure need to be within 0.5% at BSE-1 earthquakes. Therefore, 120 viscous fluid dampers are added to the structure to achieve this design objective.

This adopted device configuration in the actual building is shown in Table 4 as Configuration I, also as the existing configuration. In the device row of the table, “6A” means that six pairs of type “A” dampers are installed on the first floor between the ground and upper floor. Note that this configuration was designed using the general practice approach, where the amount of damping is the major concern. Also, the designer of this configuration considers a proportional relationship between the story damping distribution and story stiffness. This consideration is reasonable for making the supplemental damping effect as close as possible to an equivalent proportional damping.

The viscous device distribution in the floor plan is symmetrical with respect to the center. Therefore, in Table 4 the east wing and west wing have the same number of devices. At each location the dampers are placed as braces in the floor plan. Because the structure is simplified into a lumped mass model, the devices are lumped together as well.

Configuration I exhibits good results with respect to seismic response reduction. The natural frequencies of the structure have not changed much but the effective damping

Table 4. Device configuration I

location (dof-dof)	G-1	1-2	2-3	3-4	4-5	5-6	6-7	7-8	8-9	9-10	10-11
Device	6A	4A	4A	4A	2A	2A	2A	2B	2B	2B	0
location (dof-dof)	G-12	12-13	13-14	14-15	15-16	16-17	17-18	18-19	19-20	20-21	21-22
Device	6A	4A	4A	4A	2A	2A	2A	2B	2B	2B	0

Note: $A=1.4 \times 10^7$ Ns/m (80 kip.s/in), $B=0.7 \times 10^7$ Ns/m (40 kip.s/in), and $C=1.05 \times 10^7$ Ns/m (60 kip./in).

ratio is raised from 3% structural damping to 20.2%. The damping ratios for the first 20 modes are plotted in Figure 10. The maximum response of the structure with device configuration I is shown in Table 5, also plotted in figures 11–13 by solid lines.

We see from the table and figures that under the modified El Centro earthquake, the largest maximum story drift among all the stories is reduced from 46.7 mm to 19.0 mm, with a reduction ratio of 59.2%. The reduction ratio for the maximum roof displacement and the maximum absolute acceleration among all the stories are 56.8% and 81.7%, respectively. For the Kobe earthquake, the drift, roof displacement, and absolute acceleration are reduced by 76.8%, 65.9%, and 81.1%, respectively. The reduction ratios are 51.9%, 49.1%, and 82.4%, respectively, for the Northridge earthquake.

However, this configuration may not be optimal given the same number of damping devices. First, the effective damping ratio may not be the maximum. Second, even if the maximum effective damping is achieved, it may not offer the optimal response reduction, especially for a particular performance index. It is known that the added EDDs

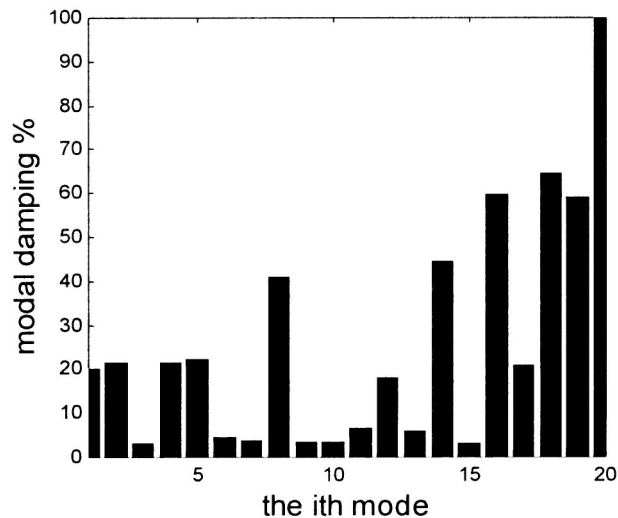
**Figure 10.** The damping ratio of the first 20 modes for device configuration I on structure.

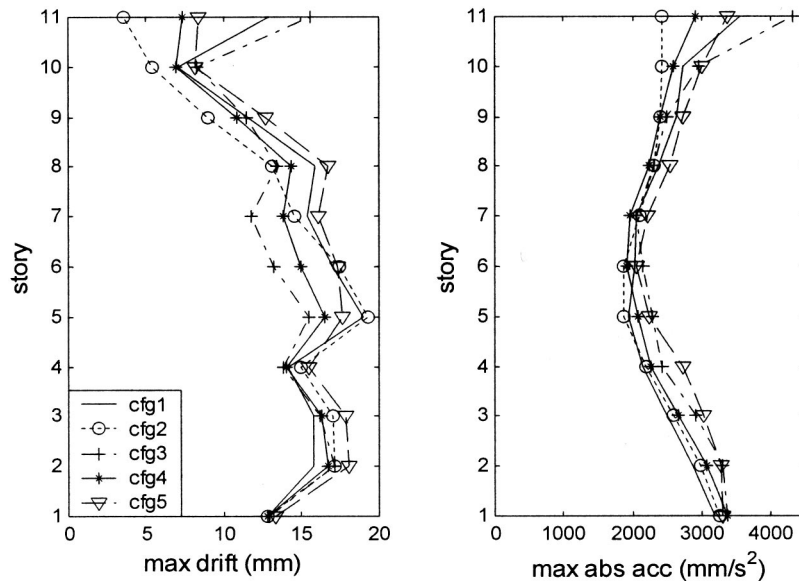
Table 5. Maximum structural response with or without Configuration I

	No damper			With damper configuration I		
	El			El		
	Centro	Kobe	Northridge	Centro	Kobe	Northridge
Drift (mm)	46.66	66.43	48.58	19.02	15.39	23.36
Roof displacement (mm)	314.18	316.98	306.85	135.64	109.76	156.18
Abs. acceleration (mm/s^2)	19505	21770	19440	3562	4103	3415

change not only the effective damping but also the other properties, such as mode shapes, modal frequencies, and modal contribution factors. Therefore, by only increasing the effective damping, the response reduction is not guaranteed to be optimal. To investigate these issues, Configuration I is optimized in the next section and four other configurations are derived.

OPTIMIZATION OF THE EDD CONFIGURATION

To optimize the existing device configuration I based on a given performance index, a modal analysis of the structure system is first considered. The indexed response is then analyzed and the dominant modes are identified. The effectiveness of each device loca-

**Figure 11.** Response of structure with device configurations under modified El Centro.

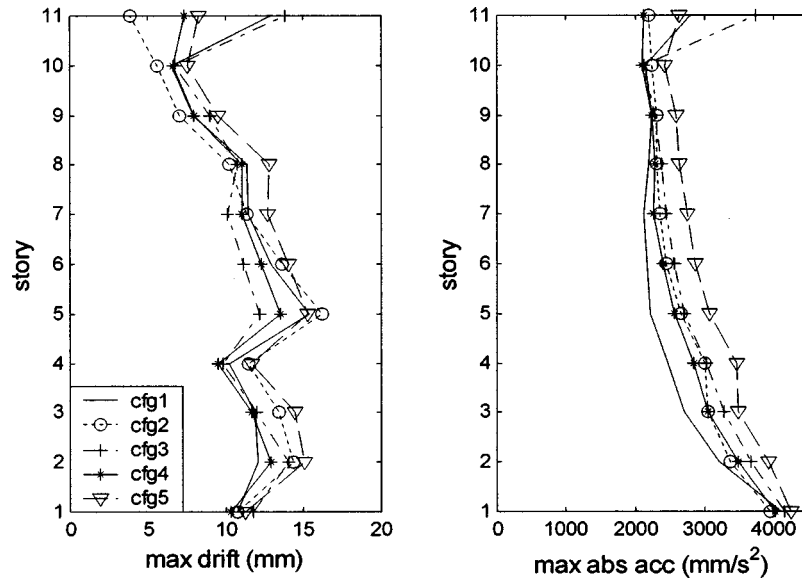


Figure 12. Response of structure with device configurations under modified Kobe.

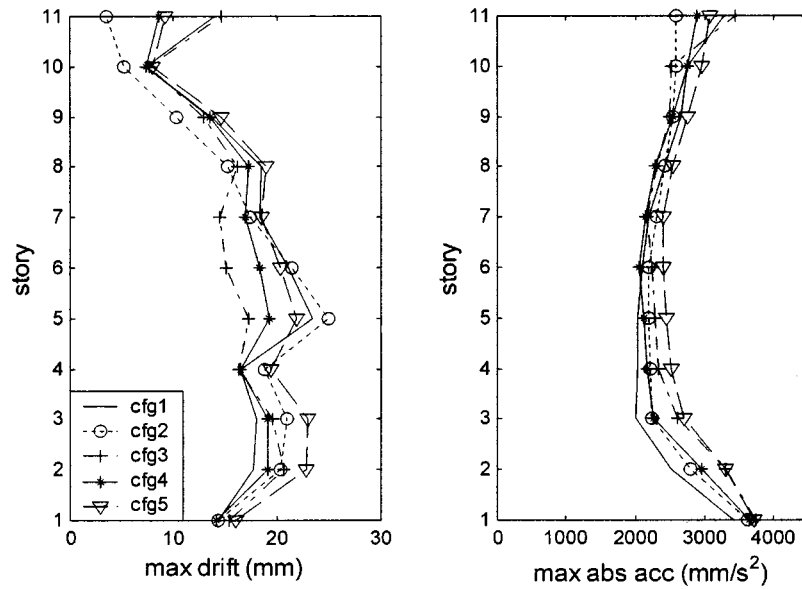


Figure 13. Response of structure with device configurations under modified Northridge.

tion is obtained by sorting its contribution to the dominant modes. Then the devices are removed from the least effective location and placed in the most effective location. The adopted procedure is explained as follows.

For a structural system subjected to earthquake excitation, it is commonly modeled as a multi-degree-of-freedom (MDOF) system. The equation of motion can be written as

$$M\ddot{U} + C\dot{U} + KU = -M\iota\ddot{U}_g = P(t), \quad (4)$$

where M , C , and K denote mass, damping, and stiffness matrices, respectively. U is the relative displacement vector. The influence vector ι represents the displacement of the masses resulting from the static application of a unit ground displacement. The response vector U can be expressed in the frequency domain as

$$U(\omega) = -H(\omega) * M\iota * A_g(\omega) \quad (5)$$

$$H(\omega) = (-M\omega^2 + i\omega * C + K)^{-1} \quad (6)$$

$H(\omega)$ is the transfer function of a structural system. The structural response to the earthquake can be obtained by the inverse transformation of $U(\omega)$.

$$U(t) = \frac{1}{2\pi} \int_{-\infty}^{\infty} U(\omega) e^{i\omega t} dt \quad (7)$$

The transfer function $H(\omega)$ reaches its maximal when frequency ω is close to one of its roots. These roots correspond to the natural frequencies of the modes. From analyzing the transfer function of one particular response quantity, the dominant mode for that quantity can be found. We can also find the modes that do not dominate the transfer function but can be excited by the earthquake, since the earthquake ground motions may contain a wide spectrum of frequency components.

First, the performance index is taken as the story drift. From the response of the structure with Configuration I (in figures 11–13), the maximum story drift occurs around the fifth story. The minimum story drift occurs at the tenth story. For the absolute acceleration response, the maximum occurs at the first and the eleventh stories, and the minimum occurs at the fifth story. In order to analyze these response quantities and further control them, the transfer functions for these quantities are plotted in figures 14 and 15.

From the transfer function of the story drift we see that the first mode dominates the transfer function for drift responses. The value of the transfer function reaches its maximum at the natural frequency of the first mode (0.66 hZ). For the other frequencies the value is small or close to zero. Because the design objective is to reduce the largest story drift, the transfer function on the fifth story is examined. It can be seen that the transfer function has large values only over a certain range. We can reduce the transfer function magnitude in that range and in turn reduce the magnitude of the frequency response of the fifth story drift. The time domain response will also be reduced. Therefore, the intermediate objective becomes the reduction of the transfer function magnitude of fifth story drift at the structure's first natural frequency. This can be done by increasing the modal damping or changing the mode shapes.

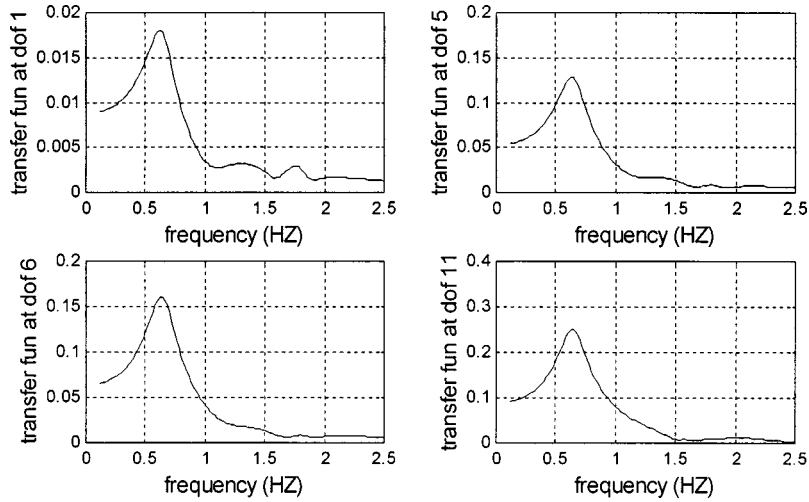


Figure 14. Drift transfer function for structure with Configuration I.

Since mode shape changes due to the addition of the devices are not straightforward, we start with modal damping. For the linear viscous device used in this structure, effective damping or the first modal damping defined in Equation 1b gives information about the device location and its corresponding contribution to the modal damping. If the devices are placed at a location with larger first-mode relative displacement between stories, the first modal damping ratio is increased more effectively than in a configuration where the devices are placed at locations with smaller first-mode relative displacement.

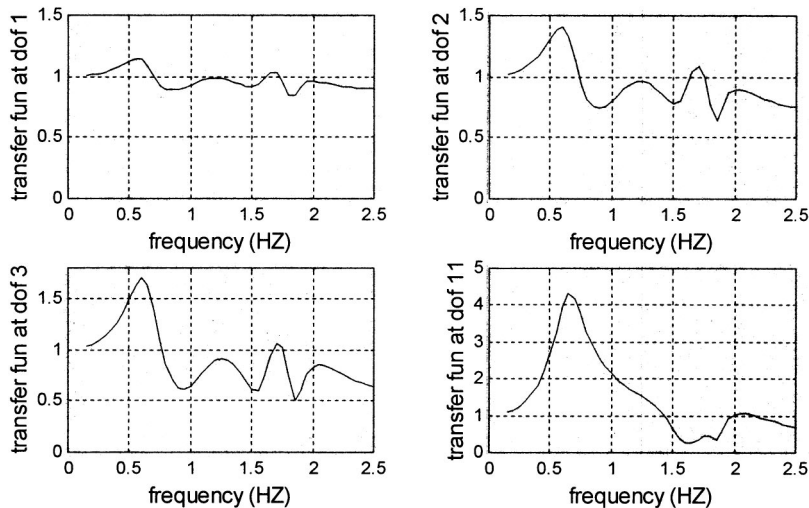


Figure 15. Absolute acceleration transfer function for structure with Configuration I.

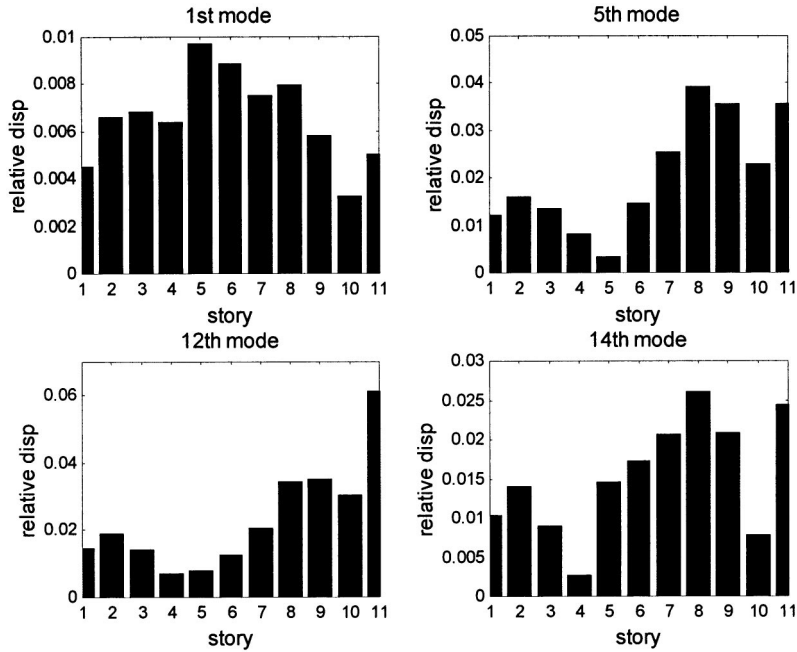


Figure 16. Modal relative displacement for each story (with Configuration I).

The first-mode relative displacements between stories are plotted in Figure 16. Note that, among the possible device locations (from first story to eleventh story), the fifth story has the largest first-mode relative displacement. Consequently, the viscous device placed at the fifth story will be most effective and devices at the first and tenth story will be least effective. Therefore, the strategy is to remove devices from the least effective stories and place them on the most effective story. In this case, because the drift response is dominated by the first mode, the optimization strategy coincides with the heuristic in the sequential approach, which places the devices at the location with the largest story drift under earthquake condition. Using this strategy as an engineering judgment, we can obtain several potential configurations. Among them, Configuration IV in Table 6 represents the best drift response reduction. And Configuration III represents the case of largest damping ratio for the fundamental mode, where we intentionally add additional 7% damping devices to the structure. The damping coefficient at each story is plotted in Figure 17 for these configurations.

A similar procedure is applied when the performance index is acceleration instead of story drift. From the transfer function of absolute acceleration (in Figure 15), we know that the frequency composition of the absolute acceleration response is much more complicated than the drift response. Although the first mode is still an important part of the response composition, the transfer function magnitudes at the natural frequencies of the higher modes are comparable to the contribution from the first mode. This is especially true for the first and second story, where the absolute accelerations are large. The sig-

Table 6. Optimized device configurations

location (dof-dof)	G-1	1-2	2-3	3-4	4-5	5-6	6-7	7-8	8-9	9-10	10-11
cfg II	2A	2A, 1B	2A, 1B	2A, 1B	2A, 1B	2A, 1B	2A, 1B	2A, 1B	2A, 1B	2A, 1B	2A, 1B
cfg III	0	2A	5A	5A	6A	5A	3A	2C	1C	1C	0
cfg IV	1A	4A	4A	4A	5A	3A	2A	2C	1A	1C	1C
cfg V	0	2B	2A	4C	5A	4C	2A	2C	1C	1C	1C

location (dof-dof)	G-12	12-13	13-14	14-15	15-16	16-17	17-18	18-19	19-20	20-21	21-22
cfg II	2A	2A, 1B	2A, 1B	2A, 1B	2A, 1B	2A, 1B	2A, 1B	2A, 1B	2A, 1B	2A, 1B	2A, 1B
cfg III	0	2A	5A	5A	6A	5A	3A	2C	1C	1C	0
cfg IV	1A	4A	4A	4A	5A	3A	2A	2C	1C	1C	1C
cfg V	0	2B	2A	4C	5A	4C	2A	2C	1A	1C	1C

nificant higher modes are fifth mode (natural frequency 1.46 HZ), twelfth mode (natural frequency 1.78 HZ), and fourteenth mode (natural frequency 1.93 HZ). These three modes can be excited by earthquakes, and therefore become significant components of the structure's response. The modal relative displacement for these modes is plotted in Figure 15. Among all the stories, eighth, eleventh, and other upper stories are more ef-

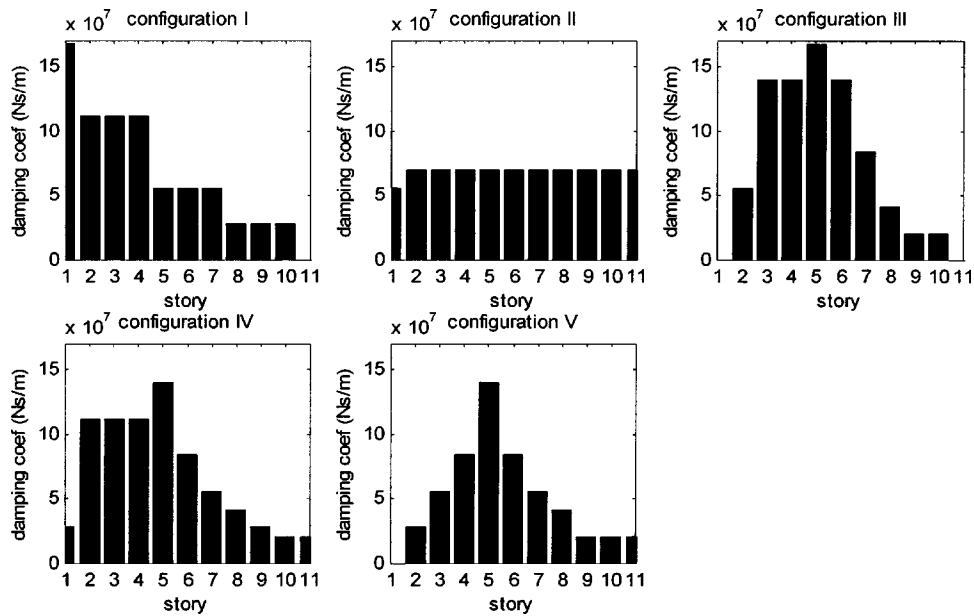
**Figure 17.** Device damping coefficient at each story for configurations I to V.

Table 7. Damping effect of configurations I, II, III, and IV

	Total damping coef (10^6 Ns/mm)	1st modal damping ratio %	5th modal damping ratio %	12th modal damping ratio %	14th modal damping ratio %	Drift reduction ratio %	Abs acc reduction ratio %
Cfg I	756	20.18	22.22	17.92	44.52	— — —	— — —
Cfg II	756	19.39	16.93	42.85	51.92	-4.4	2.0
Cfg III	812	26.71	22.33	13.09	47.1	10.0	-10.6
Cfg IV	756	23.78	22.41	19.09	44.06	14.1	0.4
Cfg IV	553	19.24	15.10	14.52	39.44	2.5	-2.5

Note: Reduction ratio is based on reduction from response of structure with Configuration I, averaged on three design earthquakes. The minus sign means the response is actually increased.

fective for the modal damping of these three higher modes. Therefore, these locations should have more devices to control the higher mode. To control the first mode, placing the device at middle and lower stories is more effective. Therefore, Configuration II is selected by placing the devices almost uniformly, with fewer devices at the first story.

Now assume the performance index is taken as the cost of the device, but the performance requirement on the story drift still needs to be met. To accomplish this, the devices are removed from the least effective locations for the drift response, e.g., first, second, and third stories. The optimized device configuration is shown in Table 6 as Configuration V. The damping coefficients for each story are plotted in Figure 17. The total damping coefficient is reduced by 26%.

RESULTS FOR THE OPTIMIZED CONFIGURATIONS

The story drift and absolute acceleration of the structure with the five device configurations are shown in figures 11 to 13. Tables 7 and 8 list the effects of different device configurations on the structure.

Among the five different device configurations, configurations II and IV have the same total damping as Configuration I, which is the existing design adopted in the actual structure. After optimization, Configuration II has the best acceleration response and IV

Table 8. Control effect of configurations I, II, III, and IV

Cfg	El Centro				Kobe				Northridge			
	Max drift (mm)	Max abs acc (mm/s^2)	Ave drift (mm)	Ave abs acc (mm/s^2)	Max drift (mm)	Max abs acc (mm/s^2)	Ave drift (mm)	Ave abs acc (mm/s^2)	Max drift (mm)	Max abs acc (mm/s^2)	Ave drift (mm)	Ave abs acc (mm/s^2)
I	19.02	3562	14.30	2543	15.39	4099	11.25	2579	23.36	3415	16.61	2489
II	19.29	3261	13.12	2401	16.21	3945	10.73	2715	24.86	3622	15.65	2519
III	17.10	4314	13.60	2779	14.10	4151	11.07	2942	20.64	3737	15.47	2677
IV	16.66	3359	13.17	2492	13.48	4006	10.40	2671	19.19	3649	15.47	2527
V	18.09	3376	14.73	2774	15.29	4253	12.08	3098	22.92	3724	17.49	2799

has the best drift response. Configuration III has the largest effective damping because it has 7% more damping devices than Configuration I. Configuration V has 26% less total damping than Configuration I.

Although Configuration III achieves the largest effective damping (i.e., first-mode damping ratio), it does not achieve the best control effect for performance indices as story drift nor absolute acceleration. If the performance index is taken as the largest story drift among all stories, Configuration IV offers the best control effect. Compared to the response of the structure in Configuration I, Configuration IV offers a 14% reduction in the largest maximum story drift among all stories. Although Configuration III also offers a 10% reduction ratio for drift, this configuration increases the absolute acceleration by 10%. This effect may be undesirable for the structure, since absolute acceleration is related to the base shear of the structure.

If the performance index is taken as the absolute acceleration, the best control effect is provided by Configuration II. Although Configuration IV is the most effective in reducing the story drift compared to Configuration I, it actually increases the acceleration by 4% in the average of three design earthquakes. Compared to Configuration I, Configuration II offers an additional 2% reduction in the largest absolute acceleration. This reduction of absolute acceleration is more obvious in the higher stories, where the story stiffness is small. Note Configuration II increases the story drift by 4.4%. This is because the absolute acceleration response and story drift response have different compositions, which are contributed by different modes. For absolute acceleration, almost every device location contributes to the modal damping of the participating modes. With an almost uniform distribution of the devices, we can obtain the best performance with respect to the maximum and average absolute acceleration.

Although the average reduction ratio obtained from Configuration II is not significant, we must note that the reduction is 8% under the El Centro earthquake, while there is an increase under the Northridge earthquake. The reason is that the maximum acceleration occurs at the eleventh story under the El Centro earthquake, while the maximum occurs at the first story under the Kobe and Northridge earthquakes. Configuration II can reduce the transfer function magnitude for the eleventh story, but it also increases the transfer function for the first story. Furthermore, this configuration may reduce one peak magnitude while at the same time increase some other peak magnitudes. This further explains that acceleration response is more complicated than drift and more tradeoffs have to be considered. The earthquake frequency content can also have a large effect on the optimal damper distribution.

If the performance index is taken as the cost with the same story drift requirement, Configuration V offers the same drift response level as Configuration I, and 26% reduction on total damping coefficient. However, the absolute acceleration response is increased. If the structural response with Configuration I reaches the performance objective and the absolute acceleration is not a stringent requirement, Configuration V can save on the cost by 26%, assuming the cost of the device is proportional to the total damping coefficient.

It is interesting to note that both configurations III and V have no device on the first story. The reason is that the first story is very stiff (with several reinforced concrete col-

umns) and the relative velocity at the first story is small. Therefore, adding dampers to this story will not have a significant amount of control force. Also, adding dampers only to other stories will not cause a soft story because the dampers do not have stiffness, they are used mainly to reduce the drift. In the case that plastic hinges occur at the first story, it is not the coverage of this study.

For other performance indices (e.g., relative acceleration, relative velocity, relative displacement, or base shear), the optimal distribution can be determined in a similar manner, considering the structural characteristic and the particular performance index.

DISCUSSION AND CONCLUSIONS

In this study, the design procedures specified by the current design provisions for building with added EDDs are reviewed. Several procedures use effective damping ratio as an indication of reduced force and deformation due to the added damping. This approach can achieve acceptable building performance. However, the configuration of damping devices is not guaranteed to be optimal. Such an approach may result in increased responses for some performance indices. A case study is used to illustrate that device configuration can be optimized for the required performance index. Through optimization of the device configuration, the seismic risk to the building and the resulting hazard to public safety (i.e., falling glass) is reduced. Cost may also be reduced because the optimal configuration may need fewer damping devices.

In the case study, five device configurations are evaluated. Configuration I, the existing design, offers the structure with acceptable performance with respect to the story drift performance index and absolute acceleration index. It is not the optimal design, however. In order to obtain the optimal control effect, the dynamic properties of the system have to be analyzed and the devices need to be redistributed to the stories that are more effective in reducing the indexed response. Among the other four redesigned configurations, Configuration III offers the largest effective damping but not the best response reduction for either drift or acceleration performance indices. Configuration IV is found to be optimal for story drift performance index, and Configuration II is optimal for absolute acceleration. Configuration V offers 26% cost savings with the same story drift response. Although these configurations are superior after several iterations, the global optimum cannot be obtained without enumerating all the possibilities. And it is expected that the optimal configuration may not be unique.

To optimize the damping device configuration, we use the modal damping ratio as a direction to reduce the structural response under earthquake vibrations. The effectiveness of each location is determined by ranking its contribution to the damping of participating modes. Then the devices are placed strategically to increase the modal damping and therefore reduce the indexed response. With this approach, the optimization is more effective than we can achieve by random trial and error. However, the modal damping is not the only indication of response reduction. The structural seismic response is also affected by many other factors, such as mode shapes, natural frequencies, and earthquake compositions. The changes in device configuration may also bring undesirable changes to the other factors. Therefore, iterations are necessary to find the optimal con-

figuration using this engineering judgment. The authors also developed an automate procedure called performance-based heuristic optimization, which obtains the optimized configuration directly. The procedure will be published later.

In this study, the optimization methodology relies on the modal analysis and structural transfer function, which provide meaningful information for linear systems. Therefore, this methodology is limited to elastic structures with dampers. Considering that dampers are added to buildings to reduce the seismic demand so that structures can remain linear, this methodology is applicable for most situations. For structures with nonlinear responses, the effects from the supplemental dampers vary, because of the energy dissipated by the structural hysteretic behaviors. These nonlinear effects are still under investigation. In addition, since most of the dampers can be simulated by equivalent linear damper, this optimization methodology is not limited to linear dampers. The effect of sublinear or other types of dampers is not covered in this study.

This study determined that the optimal configuration is highly dependent on the performance index selected. Different performance indices may lead to different optimal device configurations. Also, the optimal EDD configuration is usually specific to the structure. There are no generic rules for optimal device configuration and for multiple performance indices. The structure needs to be analyzed carefully and the response with respect to the selected performance index needs to be studied. Only experience in analyzing various types of buildings for different performance indices can provide the insight needed to establish a specific strategy for a given situation based on structural dynamics principles.

ACKNOWLEDGMENT

The authors express their sincere appreciation to the National Science Foundation for its financial support to this study through the Multidisciplinary Center for Earthquake Engineering Research (Grant No. EEC-9701471).

REFERENCES

- Agrawal, A. K., and Yang, J. N., 1998. Optimal placement of energy dissipative systems using combinatorial optimization, ASCE, *Proceedings of the Structural Engineers World Congress, July 18–23, 1998, San Francisco, CA*, Paper No. T167-3.
- American Society of Civil Engineers (ASCE), 1998. *Minimum Design Loads for Buildings and Other Structures, ASCE 7-98*, New York.
- American Society of Civil Engineers (ASCE), 2000. *Prestandard and Commentary for the Seismic Rehabilitation of Buildings, FEMA-356*, prepared for the SAC Joint Venture, published by the Federal Emergency Management Agency, Washington, D.C.
- Applied Technology Council (ATC), 1997. *NEHRP Guidelines for the Seismic Rehabilitation of Buildings, FEMA-273*, prepared for the Building Seismic Safety Council, published by the Federal Emergency Management Agency, Washington, D.C.
- Building Seismic Safety Council (BSSC), 2001. *NEHRP Recommended Provisions for Seismic Regulations for New Buildings and Other Structures, Pt. 1: Provisions, FEMA-368*, published by the Federal Emergency Management Agency, Washington, D.C.
- Chang, K. C., Soong, T. T., Oh, S.-T., and Lai, M. L., 1995. Seismic behavior of steel frame

- with added viscoelastic dampers, *J. Struct. Eng.* **121** (10), 1418–1426.
- Constantinou, M. C., and Tadjbakhsh, I. G., 1983. Optimum design of first story damping systems, *Computers and Structures* **17** (2), 305–310.
- De Silva, C. W., 1981. An algorithm for the optimal design of passive vibration controllers for flexible systems, *Journal of Sound and Vibration* **74** (4), 495–502.
- Gluck, N., Reinhorn, A. M., Gluck, J., and Levy, R., 1996. Design of supplemental dampers for control of structures, *J. Struct. Eng.* **122** (12), 1394–1399.
- Gurgoze, M., and Muller, O. C., 1992. Optimal positioning of dampers in multi-body systems, *Journal of Sound and Vibration* **158** (3), 517–530.
- Hahn, G. D., and Sathivageeswarm, K. R., 1992. Effects of added-damper distribution on the seismic response of buildings, *Computers and Structures* **43** (5), 941–950.
- Lopez Garcia, D., 2001. A simple method for the design of optimal damper configurations in MDOF structures, *Earthquake Spectra* **17** (3), 387–398.
- Miyamoto, H. K., and Scholl, R. E., 1996. Design of steel pyramid using fluid viscous dampers with moment frames, *Proceedings, 1996 Tall Buildings Conference, Los Angeles, CA*.
- Shukla, A. K., and Datta, T. K., 1999. Optimal use of viscoelastic dampers in building frames for seismic force, *J. Struct. Eng.* **125** (4), 401–409.
- Singh, M. P., and Moreschi, L. M., 1999. Genetic algorithm-based control of structures for dynamic loads, *IA-99 Proceedings of International Seminar on Quasi-Impulsive Analysis, Osaka Univ., Osaka, Japan*.
- Singh, M. P., and Moreschi, L. M., 2001. Optimal seismic response control with dampers, *Earthquake Eng. Struct. Dyn.* **30**, 553–572.
- Spencer, Jr., B. F., Suhardjo, J., and Sain, M. K., 1994. Frequency domain optimal control strategies for aseismic protection, *J. Eng. Mech.* **120** (1), 135–157.
- Takewaki, I., 1997. Optimal damper placement for minimum transfer functions, *Earthquake Eng. Struct. Dyn.* **26** (11), 1113–1124.
- Tsuji, M., and Nakamura, T., 1996. Optimal viscous dampers for stiffness design of shear buildings, *The Structural Design of Tall Buildings* **5**, 217–234.
- Wu, B., Ou, J.-P., and Soong, T. T., 1997. Optimal placement of energy dissipation device for three dimensional structures, *Eng. Struct.* **19**, 113–125.
- Zhang, R.-H., and Soong, T. T., 1992. Seismic design of viscoelastic dampers for structural applications, *J. Struct. Eng.* **118** (5), 1375–1392.

(Received 3 May 2002; accepted 29 May 2003)